Advances in Nano Research, *Vol. 3, No. 1 (2015) 13-27*
DOI: http://dx.doi.org/10.12989/anr.2015.3.1.013

Interband optical properties in wide band gap group-III nitride quantum dots

K. Jaya Bala[1a] and A. John Peter[*2]

[1]*Department of Physics, GTN Arts College, Dindigul-624 005, India*
[2]*P.G & Research Department of Physics, Government Arts College, Melur-625 106, Madurai, India*

(Received November 4, 2014, Revised March 23, 2015, Accepted March 26, 2015)

Abstract. Size dependent emission properties and the interband optical transition energies in group-III nitride based quantum dots are investigated taking into account the geometrical confinement. Exciton binding energy and the optical transition energy in $Ga_{0.9}In_{0.1}N/GaN$ and $Al_{0.395}In_{0.605}N$ /AlN quantum dots are studied. The largest intersubband transition energies of electron and heavy hole with the consideration of geometrical confinement are brought out. The interband optical transition energies in the quantum dots are studied. The exciton oscillator strength as a function of dot radius in the quantum dots is computed. The interband optical absorption coefficients in GaInN/GaN and AlInN/AlN quantum dots, for the constant radius, are investigated. The result shows that the largest intersubband energy of 41% (10%) enhancement has been observed when the size of the dot radius is reduced from 50 Å to 25 Å of $Ga_{0.9}In_{0.1}N/GaN$ ($Al_{0.395}In_{0.605}N$ /AlN) quantum dot.

Keywords: oscillator strength; exciton; quantum dot

1. Introduction

Semiconducting quantum dots are given a great deal of interests due to their unique opto-electronic properties which can be optimized by tailoring their band gaps. Their exotic electrical and optical behaviour can be applied for fabricating micro and opto-electronic devices (Bhattacharya *et al*. 2004, Sun *et al*. 2009, Teleb *et al*. 2011).The band gap can be tuned by doping suitable impurities, changing dot radius, altering barrier height of the material and applying of some external perturbations. Semiconductor quantum dot lasers, with the high differential gain and the femto-second pulses with a wide range of wavelength, are achieved (Matthews *et al*. 2002). The review on carbon nanotubes and their electronic and optical properties has been brought for the potential applications on photovoltaic devices very recently (Castrucc 2014). In a quantum dot, the charge carriers are confined in all the directions providing the quantization of electronic energy states with the discrete energy-levels which result the photons with suitable energy causing the intersubband/interband optical transitions involving large electric dipole moments (Kuhn *et al*. 1991). Quantum computing with the application of electric field to quantum dots in which the

∗Corresponding author, Professor, E-mail: a.john.peter@gmail.com
[a]Ph.D. Student, E-mail: balajmv77@gmail.com

http://www.techno-press.com/?journal=anr&subpage=7 ISSN: 2287-237X (Print), 2287-2388 (Online)

spins of confined carriers are considered to be important candidates and the recent developments of spin based quantum computing have been reviewed recently (Meighan *et al*. 2014).

Intersubband and interband optical transition energies are given quite attention, theoretically and experimentally, in recent years. Group-III nitride based semiconducting laser diodes make impact on fundamental research works and industrial research purposes in order to develop the requirements. Optical absorption experiment is one of the simple methods which can be applied directly to characterize any material. Intersubband optical absorption, in low dimensional semiconductors, has been demonstrated earlier and the optical properties are found to be essential for fabricating some novel devices such as far-infrared detectors and quantum cascade lasers, electro-optical modulators and optical switches (Kuhn *et al.* 1991, Meighan *et al*. 2014, Liu 1999). It has been proven that the interband optical transitions are capable for opto-electronic devices in the mid and far infrared spectral regions. The electronic and optical properties of self-assembled InN based quantum dots have been investigated using combined atomistic tight-binding and full configuration interaction calculations (Köhler *et al.* 2002). The exciton energies and probabilities of radiative transition from exciton state in GaN/AlN quantum dots have been computed taking into consideration of the electric field conditioned by strain induced and spontaneous polarization using the tight binding approximation (Haun and Koch 2994). The electronic and optical properties of wurtzite and zinc-blende GaN/AlN quantum dots have been studied theoretically and found that the strain field strongly modifies the excitonic states in both wurtzite and zinc-blende GaN/AlN quantum dots (Fonoberov and Balandin 2004). Radiative lifetime of excitons in ZnO nanocrystals has been discussed with the geometrical confinement effect (Fonoberov and Balandin 2004, 2006).

Wide-band-gap wurtzite nanocrystals, such as ZnO and GaN quantum dots, have been given attention for the potential applications in fabricating optoelectronic, electronic, and biomedical applications (Fonoberov *et al.* 2006). Electrically or optically pumping semiconductor intersubband lasers on terahertz emission in reduced dimensional semiconductors have been discussed earlier (Tchelidze and Tkreselidze 2004, Liu *et al*. 2004, Cao *et al.* 2001, Qu and Morais 2003). Further, the intersubband optoelectronics are utilized for the development of ultrafast photonic devices for optical telecommunication systems. GaN based wide band gap semiconductors are well suitable materials for fibre optics transmission windows between 1.3 μm and 1.55 μm because group-III nitride heterostructure semiconductors having larger conduction band offsets to accommodate intersubband optical transition energies. The room temperature intersubband photoluminescence based on the GaN wide band gap low dimensional semiconducting materials operating at wave lengths 1.55 μm has been observed earlier (Levou *et al.* 2007, 2008). Effects of contact space charge on the performance of quantum intersubband photo-detectors have been developed to demonstrate the effect of the non-uniform field on the photo-detector operation (Barve *et al.* 2012) Intersubband absorption properties of high Al content AlGaN /GaN multiple quantum wells grown with different interlayers by metal organic chemical vapor deposition have been studied earlier (Sun *et al*. 2012).

In the present work, the exciton binding energy and the optical transition energy in $Ga_{0.9}In_{0.1}N$/GaN and $Al_{0.395}In_{0.605}N$ /AlN quantum dots are discussed taking into consideration of spatial confinement. The largest intersubband transition energies of electron and heavy hole with the consideration of geometrical confinement are discussed. The exciton oscillator strength, as a function of dot radius in these quantum dots, is found. The optical absorption coefficients, in GaInN/GaN and AlInN/AlN quantum dots for the constant radius 20Å, are investigated. The interband optical transition energies in the quantum dots are computed. The paper is organized as

follows. In Section 2, the theoretical model used in our calculations of obtained confined binding energies of exciton, and the interband optical properties are brought out. The results and discussion are presented in Section 3. A brief summary and results are presented in the last Section.

2. Model and calculations

2.1 Exciton binding energy

Within the framework of effective mass approximation, the Hamiltonian of a confined exciton in a cylindrical wurtzite group-III nitride based semiconductor quantum dot is considered in this problem. The cylindrical dot is characterized with the radius R and height L along z-direction. The exciton which consists of a single electron part (H_e), the single hole part (H_h) and Coulomb interaction term between electron-hole pair is given by

$$\hat{H}_{exe} = H_e(\bar{r}_e) + H(\bar{r}_h) - \frac{e^2}{\varepsilon_0 |\bar{r}_e - \bar{r}_h|} \tag{1}$$

where e is the absolute value of electron charge, $|\bar{r}_e - \bar{r}_h|$ denotes the relative distance between the electron and the hole and ε_0 is the dielectric constant of the material. $Ga_xIn_{1-x}N/GaN$ and $Al_xIn_{1-x}N/AlN$ materials are taken as quantum dots in this paper with the same barrier height. The present problem involves some group-III nitride wide band gap semiconductors such as GaN, AlN and InN. They are direct band gap semiconducting materials and their conduction band minima lie at the Γ valley.

The Hamiltonian of the exciton confined in the strained quantum dot in the cylindrical coordinates is written as

$$H_j = -\frac{\hbar^2}{2m_j^*}\left[\frac{1}{\rho_j}\frac{\partial}{\partial\rho_j}\left(\rho_j\frac{\partial}{\partial\rho_j}\right) + \frac{1}{\rho_j^2}\frac{\partial^2}{\partial\phi_j^2} + \frac{\partial^2}{\partial z_j^2}\right] + V(\rho_j, z_j) \mp eFz_j - \frac{e^2}{\varepsilon_0 |z_e - z_h|} \tag{2}$$

where j=e and h refer to the electron and hole respectively, $V(\rho_j, z_j)$ is the electron (hole) confinement potential due to the contribution from the barrier material including the strain effect ($V_{c(v)strain}$) and the barrier offset. The sign + for the electron and – for hole with F is the built-in internal field induced by the spontaneous and piezoelectric polarizations in the group-III nitride quantum structure. e is the absolute value of electron charge and ρ_j is the in-plane co-ordinates of electron (hole). $|z_e - z_h|$ is the relative distance between the electron and the hole. Assuming the mass of the electron as isotropic and hence $m_{e\|}^* = m_{e\perp}^* = m_e^*$.The electron (hole) effective mass is given by m_j^*

$$m_j^* = \begin{cases} m_{Ij}^* & -\frac{L}{2} \le z \le \frac{L}{2} \\ m_{IIj}^* & |z| > \frac{L}{2} \end{cases} \tag{3}$$

The energy dependent effective mass is given by Voskoboynikov *et al*. (2003)

$$\frac{1}{m_e^*(E)} = \frac{1}{m_0}\frac{E_g^\Gamma(E_g^\Gamma+\Delta)}{(3E_g^\Gamma+2\Delta)}\left[\frac{2}{E+E_g^\Gamma}+\frac{1}{E+E_g^\Gamma+\Delta}\right]. \quad (4)$$

where E denotes the electron energy in the conduction band, m_0 is the conduction band effective mass, E_g^Γ and Δ are the main band gap and spin-orbit band splitting energy in the inner dot respectively.

The energy shifts of the strained conduction band and valence band are computed below. The strain-induced potential for the conduction band in the influence of respective alloy content(x), in the $Ga_xIn_{1-x}N$/GaN and $Al_xIn_{1-x}N$/AlN quantum dots, is given by Singh (1996)

$$V_{Cstrian}(x) = a_c[\varepsilon_{xx}(x)+\varepsilon_{yy}(x)+\varepsilon_{zz}(x)] \quad (5)$$

where a_c is the deformation potential constant of conduction band, x is the alloy concentration of the material i.e., Ga is the first dot material ($Ga_xIn_{1-x}N$) and Al is the second dot material ($Al_xIn_{1-x}N$), $\varepsilon_{xx}(x)=\varepsilon_{yy}(x)=\frac{a(x)-a_0(x)}{a_0(x)}$ where $a_0(x)$ and $a(x)$ are the lattice constants of inner dot and outer barrier material of the respective quantum dot. And $\varepsilon_{zz}(x) = -2\frac{C_{12}(x)}{C_{11}(x)}\varepsilon_{xx}(x)$, the interpolated values of elastic constants, $C_{11}(x)$ and $C_{12}(x)$, are shown in Table 1.

Parameter	$Ga_xIn_{1-x}N$	$Al_xIn_{1-x}N$
$E_g(eV)$	1.994(1−x)+3.507x−3.2x(1−x)	1.994(1−x)+6.23x−2.5x(1−x)
m_e^* (m_0)	0.11(1−x)+0.18x	0.11(1−x)+0.25x
m_h^* (m_0)	1.61(1−x)+1.65x	1.61(1−x)+3.68x
Δ_{SO} (eV)	0.019(1−x)+0.014x	0.019(1−x)+0.001x
ε	15.3(1−x)+8.9x	15.3(1−x)+8.4x
E_p (eV)	14.6(1−x)+14x	14.6(1−x)+14.5x
a_c (eV)	−6(1−x)−2.2x	−6(1−x)−1.85x
a_v (eV)	−3.4(1−x)−5.2x	−3.4(1−x)−1.5x
b_v (eV)	−1.9(1−x)−2.2x	−1.9(1−x)−1.2x
C_{11} (GPa)	396(1−x)+390x	396(1−x)+223x
C_{12} (GPa)	137(1−x)+145x	137(1−x)+115x
C_{13} (GPa)	108(1−x)+106x	108(1−x)+92x
C_{33} (GPa)	373(1−x)+398	373(1−x)+224
e_{13} (C/m^2)	−0.50(1−x)−0.35x	−0.50(1−x)−0.57
e_{31} (C/m^2)	−0.57(1−x)−0.49x	−0.57(1−x)−0.60x
e_{33} (C/m^2)	1.79(1−x)+1.27x	1.79(1−x)+0.97x
d_{31} (pm/V)	−2.1(1−x)−1.6x	−2.1(1−x)−3.5x
d_{33} (pm/V)	5.4(1−x)+3.1x	5.4(1−x)+7.6x
P_{sp} (C/m^2)	−0.081(1−x)−0.029x	−0.081(1−x)−0.032x

*parameters taken from the Vurgaftman *et al*. (2001).
**Wurtzite crystal structur

The strain related potential for the valence band with the incorporation of respective alloy content in these quantum dots can be written as Bir and Pikus (1974)

$$V_{Vstrain}(x) = a_v[(\varepsilon_{xx}(x) + \varepsilon_{yy}(x) + \varepsilon_{zz}(x)) - \frac{b}{2}(\varepsilon_{xx}(x) + \varepsilon_{yy}(x) - 2\varepsilon_{zz}(x)] \tag{6}$$

where a_v and b are the deformation potential constants of valence band.

The electron (hole) confinement potential, $V_j(\rho_j, z_j)$, due to the band offset between the inner dot and outer barrier dot is given by

$$V_j(\rho_j, z_j) = \begin{cases} 0 & \rho_j \leq R, \quad |z_j| \leq L/2 \\ V_j & \rho_j > R, \quad |z_j| > L/2 \end{cases} \tag{7}$$

where L is the height of the cylindrical quantum dot and R is the dot radius. The barrier height, V_j, is expressed as

$$V_j = Q_c \Delta E_g^{\Gamma} \tag{8}$$

where Q_c is the conduction band offset parameter which is taken as 75:25 between conduction band and valence band in all the cases and the ΔE_g^{Γ} is the difference between the band gaps of barrier and quantum dot materials.

Thus, the band gap, with the inclusion of strain effects, is given by

$$E_g(x) = \Delta E_g^{\Gamma} + \delta E_{HH}(x) \tag{9}$$

with the Γ valley band gap energy, within the parabolic dependence, is given by

$$E_g(x) = (1-x)E_g(D) + xE_g(B) - x(1-x)b \tag{10}$$

where the values of bowing parameters of the respective materials are given in Table 1, D denotes the dot material and the B refers the barrier material and the shift due to strain is given by

$$\delta E_{HH}(x) = \frac{1}{3}\Delta_0 - (a_c - a_v)\left(\frac{2C_{12}(x)}{C_{11}(x) + C_{12}(x)} + 2\right)\left(\frac{a_0(x) - a(x)}{a(x)}\right) \tag{11}$$

The polarization in a self formed wurzite quantum dot has both spontaneous and piezoelectric components. The piezoelectric tensor will have three independent nonvanishing components namely e_{31}, e_{33} and e_{15} (Prete *et al*. 2001). Thus the total polarization, $\vec{P}_{tot}$ is addition of spontaneous polarization $\vec{P}_{SP}$ and piezoelectric polarization $\vec{P}_{PE}$ without the application of external electric field.

The direction of built-in internal electric field depends on the orientation of the piezoelectricity and spontaneous polarization. The direction of piezoelectricity and spontaneous polarization is taken along the *z* direction. In general, these built-in internal fields are adjusted by the inner and barrier material of any heterostructure system. These interpolated expressions for the strain contribution are listed in Table 1 for all the three semiconductors taken in the problem. The spontaneous and piezo electric polarizations are expressed as Ambacher *et al*. (2002, 2001)

$$P^{SP}_{Ga_{1-x}Al_xN}(x) = -0.090 - 0.034(1-x) + 0.021x(1-x) \quad C/m^2 \tag{12}$$

$$P^{PZ}_{Ga_{1-x}Al_xN}(x) = -0.0525x + 0.0282x(1-x) \quad C/m^2 \tag{13}$$

where x is the Al concentration of GaAlN alloy compound.

The stress induced piezo electric internal field (P^{PZ}) related to mismatch between the inner dot and the outer barrier material along the z-direction is given by

$$P^{PZ}(x) = e_{33}\varepsilon_z + e_{31}(\varepsilon_x + \varepsilon_y) \tag{14}$$

where

$$e_{31} = (C_{11} + C_{12})d_{31} + C_{13}d_{33} \tag{15}$$

and

$$e_{33} = 2C_{13}d_{31} + C_{33}d_{33} \tag{16}$$

Thus, the piezoelectric polarization can be written as

$$P^{PZ}(x) = 2\frac{a_D - a_B}{a_B}\left(e_{31} - e_{33}\frac{C_{13}}{C_{33}}\right) \tag{17}$$

The values of elastic constants, C_{ij}, the piezoelectric moduli, d_{ij} and the piezoelectric constants are listed in Table 1. Thus, the total internal fields, which are related to the piezoelectric polarizations, within the quantum dot and the barrier are given by Bernardini *et al*. (1997)

$$F_{dot} = \left| -\frac{(P^{(D)}_{SP} + P^{D}_{PE} - P^{(B)}_{SP})z_B}{\varepsilon_0(2\varepsilon^{(B)}_e z_{(D)} + \varepsilon^{(D)}_e z_{(B)})} \right| \tag{18}$$

$$F_{barrier} = 2\left| \frac{(P^{(D)}_{SP} + P^{(D)}_{PE} - P^{(B)}_{SP})z_{(D)}}{\varepsilon_0(2\varepsilon^{(B)}_e z_{(D)} + \varepsilon^{(D)}_e z_{(B)})} \right| \tag{19}$$

where ε_0 is the dielectric constants of the respective materials, the superscripts, D stands for the dot material and B stands for barrier material of the quantum dot. Here, ε_e is the electronic dielectric constant of the respective materials. The direction of the built-in electric field F depends on the orientation of the piezoelectricity and spontaneous polarization. Generally, the above piezo and pyroelectric values can be obtained by the polarity of the crystal and the internal strains of the quantum heterostructure.

In general, group-III nitride semiconductors lack an inversion symmetry along the c-axis the heterostructure semiconductors will have spontaneous polarization and the piezo electric polarizations which is due to strain related to the lattice mismatch between inner and outer materials. The values of spontaneous polarization increase from GaN to InN to AlN materials in magnitude. Thus, the internal fields arise not only with the piezo electric polarization in addition to that of spontaneous polarization due to the application of stress. Pyroelectric effects are related to the change in spontaneous polarization due to the variation of temperature. Eventually, this strain

induced fields have larger values in group-III nitride materials than other III-V semiconductors due to the ionic character of III-nitride bond (Bernardini *et al*. 1997). The magnitude of the piezoelectric polarization increases with strain and in fact it enhances with the lattice mismatch. Thus, these combined polarizations, leading to a large internal electrostatic field, strongly affect the optical and electrical properties of group-III heterostructure systems. The intersubband optical transition arises due to this asymmetry between the inner and outer material of the quantum dot which is the main significance of functioning any photo-detector and optical switches. The asymmetry arises due to the lattice mismatch between the inner and outer materials, composition and the effects of strain.

The wave functions of the electron and hole confined in the quantum dot can be written as

$$\psi_j(\rho_j,\phi_j,z_j) = f(\rho_j)h(z_j)e^{-im\phi_j} \quad m = 0,\pm1,\pm2,... \tag{20}$$

where m is the electron (hole) z-component angular momentum quantum number. The radial wave function $f(\rho_j)$ and the corresponding confinement energy equation of the electron (hole) can be obtained by using the m-order Bessel function J_m and the modified Bessel function K_m. The z-axis wave function $h(z_j)$ can be found using linear combinations of analytical functions $\sin(\xi)$ and $\cos(\xi)$ (inside the dot), or $\exp(\xi)$ (outside the dot).

Considering the correlation of the electron-hole relative motion, the trial wave function can be chosen as

$$\Psi(\bar{r}_e,\bar{r}_h) = \psi_e(\rho_e,\phi_e,z_e)\psi_h(\rho_h,\phi_h,z_h)e^{-\alpha\rho^2}e^{-\beta z^2} \tag{21}$$

where ψ_e and ψ_h are electron and hole wave functions in the quantum dot respectively as in Eq. (20) in which f_e and f_h are ground state solution of the Schrödinger equation for the electrons and holes in the absence of the Coulomb interaction, given by

$$f_e(z_e) = \begin{cases} \cos(k_e z_e) & z_e \le |L/2| \\ A_e \exp(-\delta_e |z_e|) & z_e > |L/2| \end{cases} \tag{22}$$

$$f_h(z_h) = \begin{cases} \cos(k_h z_h) & z_h \le |L/2| \\ A_h \exp(-\delta_h |z_h|) & z_h > |L/2| \end{cases} \tag{23}$$

where

$$k_j = \sqrt{\frac{2m_j^* E_{nlk}}{\hbar^2}}, \tag{24}$$

and

$$\delta_j = \sqrt{\frac{2m_j^*(V - E_{nlk})}{\hbar^2}} \tag{25}$$

Using the boundary condition the lowest binding energies (E_{nlk}) are calculated. Eq. (23) describes the correlation of the electron-hole relative motion. α and β are variational parameters responsible for the in-plane correlation and the correlation of the relative motion in the z-direction

respectively (Bigenwald *et al*. 1999). By matching the wave functions and the effective mass and their derivatives at boundaries of the quantum dot and along with the normalization, we fix all the constants in the above equations except the variational parameters. These constants are obtained by the interface conditions between the dot and the barrier. So the wave function Eq. (23) completely describes the correlation of the electron-hole relative motion. It is worth noted that the two-parameter variational wave function is a good choice for obtaining the energy eigen values in wurtzite quantum dots.

The Schrödinger equation is solved variationally by finding $\langle H \rangle_{\min}$ and the binding energy of the exciton in the quantum dot is given by the difference between the energy with and without Coulomb term. The calculation of the electronic structure of the quantum dot systems for a fixed alloy content is computed first by calculating its lowest binding energy and subsequently the exciton binding energy by adding the Coulomb term. The expectation values of the Hamiltonian (Eq. (1)) calculated using a trial function with two variational parameters are minimized to obtain the ground-state energies of the heavy excitons. Then, by using the density matrix approach, within a two-level system approach, the intersubband optical transition energies and the related optical absorption coefficient are computed in saturation limit. The dependence of the nonlinear spectral processes in the presence of geometrical confinement is brought out the various photon energy.

The exciton binding energy of the system is obtained as

$$E_{exc}(x) = E_e + E_h - \left\langle H_{exc} \right\rangle_{\min}. \tag{26}$$

where $E_{e,h}$ is the sum of the free electron and the free hole self-energies in the same quantum dot.

The interband emission energy E_{ph} related with the confined exciton in the quantum dots is computed by

$$E_{ph} = E_e + E_h + E_g^{\Gamma} - E_{exc}(x) \tag{27}$$

where E_g^{Γ} is band gap energy of inner material of the quantum dot.

2.2 Absorption coefficients and refraction index changes

Investigation of some optical properties of any low dimensional semiconductor system is required for any electronic transition systems. Especially, study of absorption coefficient is an interesting feature of interband optical transitions. Intersubband switches and photodetectors are based on the intersubband absorption in any low dimensional semiconductor system. However, the dipole transition transitions are allowed using the selection rules $\Delta l = \pm 1$ where l is the angular momentum quantum number. Any transition rate from the ground state to the final state, the intersubband in the influence of electromagnetic spectrum, is described by Fermi Golden rule as

$$W_{fi} = \frac{2\pi}{\hbar^2} \left| \left\langle \psi_i \left| H' \right| \psi_f \right\rangle \right|^2 \delta(E_f - E_i - \hbar\omega) \tag{28}$$

where H' is the interaction Hamiltonian, $\hbar\omega$ is the radiation energy, ψ and E are the wave functions and energies of the confinement levels for the initial (i) and final (f) states. Smaller group-III nitride materials are required for larger intersubband transition energies and hence, the Eq. (28), in the strong confinement region, can be written as

$$W_{fi} = \frac{2\pi}{\hbar^2}\frac{e^2E_0^2}{4m_e^{*2}\omega^2}\left|\left\langle \psi_f \left|\vec{\varepsilon}.\vec{p}\right|\psi_i \right\rangle\right|^2 \delta(E_f - E_i - \hbar\omega) \tag{29}$$

The selection rules and the electric field having a component perpendicular to the semiconductor layers are taken into account for the intersubband optical transitions. In addition to that the oscillator strength which is related to the dipole transition, expressed as

$$P_{fi} = \frac{2m^*}{\hbar^2}\Delta E_{fi}\left|M_{fi}\right|^2 \tag{30}$$

where $\Delta E_{fi}=E_f-E_i$ refers the difference of the energy between the lower and upper states. $M_{fi} = 2\left\langle f\left|e\vec{R}\right|i\right\rangle$ is the electric dipole moment of the transition from i state to f state in the quantum dot. The matrix element is important for the calculation of different optical properties of the system related to the electronic transitions. The dipole moments are responsible for the different oscillatory strength for interband and intraband optical transitions. And, in fact, this dipole moment measures the oscillatory strength between two subbands leading to the linear and nonlinear response of a system. The observation of oscillator strength is imperative especially in the study of optical properties and they are related to the electronic dipole allowed absorptions. Moreover, the outcome of the results will viewed on the fine structure of the optical absorption. The optical absorption calculations are based on the Fermi Golden rule from which the total absorption coefficient is given by de Sousa *et al*. (2005)

$$\alpha(\omega, I) = \alpha_1(\omega) + \alpha_3(\omega, I) = \omega\sqrt{\frac{\mu_0}{\varepsilon_r}}\,\mathrm{Im}\left[\varepsilon_0\chi_1(\omega) + \varepsilon_0\chi_3(\omega)I\right] \tag{31}$$

where μ_0 is the permeability of the material, ε_r is the real part of the permittivity and I is the incident light intensity. $\chi_1(\omega)$ and $\chi_3(\omega)$ describe the linear and nonlinear contribution to the polarization with the same frequency of the incident field.

The optical absorption coefficient is given by

$$\alpha_1(\omega) = \frac{4\pi\alpha_f\sigma_s}{n_r e^2}\hbar\omega\left|M_{fi}\right|^2\delta(E_f - E_i - \hbar\omega) \tag{32}$$

and

$$\alpha_3(\omega, I) = -\frac{32\pi^2\alpha_f\sigma_s I}{n_r^2 e^2\hbar\Gamma_{ff}}\hbar\omega\left|M_{fi}\right|^2\delta(E_f - E_i - \hbar\omega)\left\{1 - \frac{\left|M_{ff} - M_{ii}\right|^2}{4\left|M_{fi}\right|^2}\times \frac{\left[(\hbar\omega - E_{fi})^2 - (\hbar\Gamma_{fi})^2 + 2E_{fi}(E_{fi} - \hbar\omega)\right]}{E_{fi}^2 + (\hbar\Gamma_{fi})^2}\right\} \tag{33}$$

where σ_s is electron density of the quantum dot, n_r is the refractive index of the semiconductor, ω the angular frequency of the incident photon energy, α_f is the fine structure constant and E_i and E_f denote the confinement energy levels for the ground and the first excited state, respectively. The

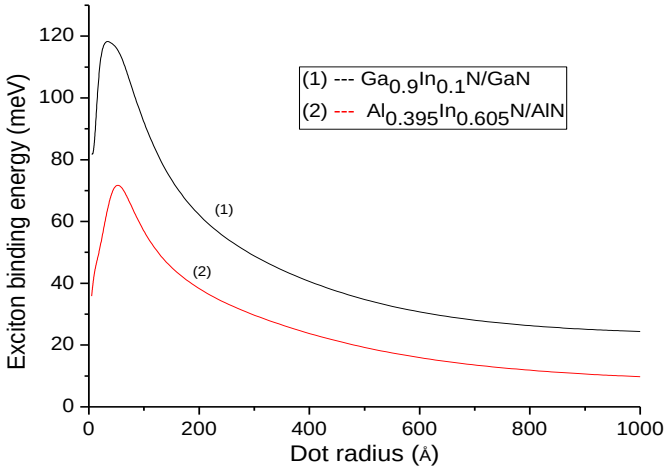

Fig. 1 Variation of exciton binding energy as a function of dot radius for $Ga_{0.9}In_{0.1}N/GaN$ and $Al_{0.395}In_{0.605}N$ /AlN quantum dots

above two equations are linear and third order nonlinear optical absorption coefficients.

From Eq. (32) and Eq. (33), the energy-conserving delta function by the Lorentzian is given by

$$\delta(E_f - E_i - \hbar\omega) = \frac{\Gamma}{\pi\left\{(E_f - E_i - \hbar\omega)^2 + \Gamma^2\right\}} \tag{34}$$

where Γ is the line width of the exciton.

3. Results and discussion

Numerical calculations are carried out to obtain the binding energy of the confined exciton and the interband optical transition energies in $Ga_xIn_{1-x}N/GaN$ and $Al_xIn_{1-x}N/AlN$ semiconductor quantum dots. The cylindrical coordinates are followed in the system and the height of the cylindrical quantum dot is taken as 50 Å throughout the paper. In general, the height of GaN based cylindrical quantum dots should be less than 50 Å due to the strong built-in electric field effect (Shi and Gan 2003). Variational formulism and the compact density matrix method are employed to obtain the electronic and optical properties of the materials. The barrier height of the confined potential is taken as 2300 meV and it is kept constant for all the three materials taken in our problem. And hence, with the concentration of Ga in the first material and Al in the second material, the quantum dots become $Ga_{0.9}In_{0.1}N/GaN$ and $Al_{0.395}In_{0.605}N$ /AlN. The effects of strain contribution from the spontaneous polarization and the piezoelectric polarization are included in the Hamiltonian. The material parameters used in our calculations are listed in Table 1 and the units of length and energy used throughout are the effective Bohr radius $R^* = \hbar^2\varepsilon/\mu e^2$ and the effective Rydberg $R_y^* = \mu e^4/2\varepsilon^2\hbar^2$ where ε is the dielectric constant and μ is the reduced mass of the exciton of the inner material.

Fig. 1 shows the variation of exciton binding energy as a function of dot radius of nitride based two different quantum structures of dots namely $Ga_{0.9}In_{0.1}N/GaN$ and $Al_{0.395}In_{0.605}N$ /AlN

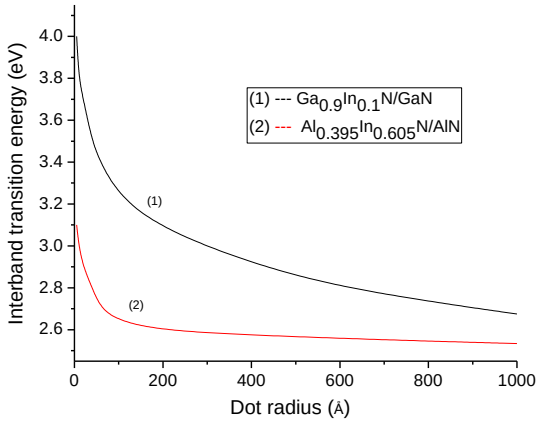

Fig. 2 Variation of optical transition energy as a function of dot radius for $Ga_{0.9}In_{0.1}N/GaN$ and $Al_{0.395}In_{0.605}N$ /AlN quantum dots

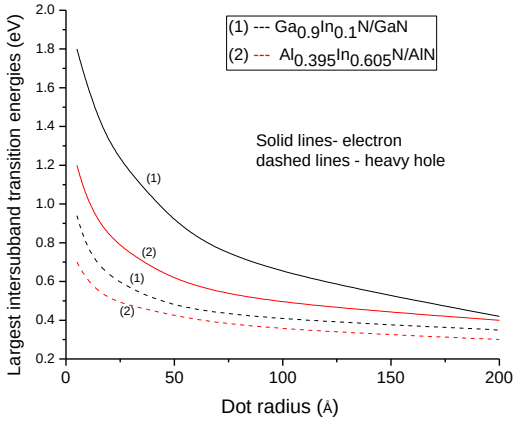

Fig. 3 Variation of the largest intersubband transition energies of electron and heavy hole as a function of dot radius for $Ga_{0.9}In_{0.1}N/GaN$ and $Al_{0.395}In_{0.605}N$ /AlN quantum dots

materials. It is observed that the exciton binding energy starts increasing when the dot radius is reduced in both the cases. It increases upto the critical radius and starts decreasing after the critical radius. The critical radius of $Ga_{0.9}In_{0.1}N/GaN$ quantum dot is found to be 32 Å whereas it is observed as 42 Å for $Al_{0.395}In_{0.605}N$ /AlN quantum dot. The reduction of exciton binding energies in the strong confinement region is the leaking of wave functions through the barrier. In that region, the exciton binding energy approaches the bulk value of the barrier. The reduction in binding energy for the larger dot radius is due to the spreading of the wave function (Wang *et al*. 2013). The bulk exciton binding energy is found to be 23 meV for $Ga_{0.9}In_{0.1}N/GaN$ quantum dot and 13 meV for $Al_{0.395}In_{0.605}N$ /AlN quantum dot. The same barrier height is taken for two quantum dots for computing the exciton binding energy and the optical transition energy.

In Fig. 2, we present the variation of interband optical transition energy as a function of dot radius for $Ga_{0.9}In_{0.1}N/GaN$ and $Al_{0.395}In_{0.605}N$ /AlN quantum dots. It is observed that the optical transition energy increases monotonically as the dot radius decreases in all the cases. This is due to the confinement of electron-hole with respect to z-plane when the cylindrical dot is increased. It is clearly shown that the effect of bound exciton has influence on the interband emission energy. This representation brings out the quantum size effect. The interband emission energy for $Ga_{0.9}In_{0.1}N/GaN$ is found to be higher compared with $Al_{0.395}In_{0.605}N$ /AlN quantum dot. It is due to the higher exciton binding energy is found to be in the $Ga_{0.9}In_{0.1}N/GaN$ quantum dot than the $Al_{0.395}In_{0.605}N$ /AlN semiconductor quantum dot (Abba and Player 2014, Renard *et al*. 2008).

The variation of largest intersubband transition energies of electron and heavy hole as a function of dot radius for $Ga_{0.9}In_{0.1}N/GaN$ and $Al_{0.395}In_{0.605}N$ /AlN quantum dots is shown in Fig. 3. This figure shows the largest intersubband transition energies between the ground state and the highest confined eigen state for electron and the heavy hole in $Ga_{0.9}In_{0.1}N/GaN$ and $Al_{0.395}In_{0.605}N$ /AlN quantum dots. The larger intersubband transitions are observed in the conduction band than the valence band. It is because the barrier height of the conduction band is higher than the valence band also this energy is found to increase as the geometrical size of the quantum dot decreases. It is because the quantum size effect dominates in this region. It is obvious that the highest

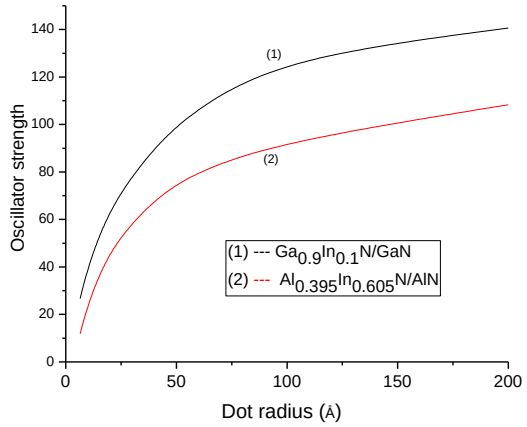

Fig. 4 Exciton oscillator strength as a function of dot radius for $Ga_{0.9}In_{0.1}N/GaN$ and $Al_{0.395}In_{0.605}N$ /AlN quantum dots

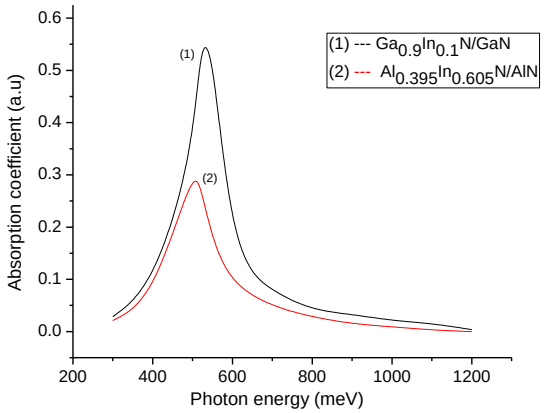

Fig. 5 Variation of absorption coefficient as a function of photon energy for $Ga_{0.9}In_{0.1}N/GaN$ and $Al_{0.395}In_{0.605}N$ /AlN quantum dots with the constant radius 20Å

intersubband transitions can be controlled and determined by the quantum confinement effects and the proper combination of the alloy concentration in the dot material. The alloy concentration determines the barrier height of any heterostructure. In addition, the intersubband transitions are found to be less for the heavy hole transitions due to the smaller confinement potential of the valence band. Thus, the desired absorption wave lengths can be obtained by having suitable semiconductors with the proper composition and the geometrical size.

Fig. 4 shows the oscillator strength as a function of dot radius for $Ga_{0.9}In_{0.1}N/GaN$ and $Al_{0.395}In_{0.605}N$ /AlN quantum dots. In absorption any spectra, the intensity of an exciton bnding energy and the envelope wave function are characterized by the oscillator strength and the expression for the oscillator strength is given by Koga *et al.* (2002)

$$f = \frac{E_p}{E_{exc}} \left| \int_V \psi_{exc}(r) d\tau \right|^2 \tag{35}$$

where E_p are the Kane energy of respective semiconductors and $d\tau$ is the volume element. It is observed that the oscillator strength increases with the dot radius whereas the transition energy decreases with the dot radius. It is because matrix element increases with the dot radius. The radiative life time can be calculated as

$$\tau = \frac{2\pi\varepsilon_0 m_0 c^3 h^2}{\sqrt{\varepsilon} e^2 E_{exc}^2 f} \tag{36}$$

where f is the oscillator strength as given in Eq. (36) , E_{exc} is the exciton binding energy and all the other parameters are universal physical constants. It is found that the radiative life time of exciton decreases with the dot radius. The spatial separation of electrons and holes allows for the formation of much stable excitons. The results pave the way for designing photo-detectors and optical switches with narrow linewidths.

Fig. 5 shows the variation of absorption coefficient as a function of photon energy for $Ga_{0.9}In_{0.1}N/GaN$ and $Al_{0.395}In_{0.605}N$ /AlN quantum dots for the constant radius 20Å . It is observed that the intersubband absorption spans the energy ranges from 450 and 600 meV for $Ga_{0.9}In_{0.1}N/GaN$ quantum dot. This absorption profile broadens for the $Al_{0.235}In_{0.765}N$ /AlN quantum dot. The resonant peak is found to be higher for $Ga_{0.9}In_{0.1}N/GaN$ quantum dot than the $Al_{0.395}In_{0.605}N$ /AlN quantum dot. This broadening feature exactly agrees well with the previous investigator (Malis *et al*. 2009). It is because the exciton binding energy and thereby the optical transition energy is higher for $Ga_{0.9}In_{0.1}N/GaN$ quantum dots compared with the other semiconductor quantum dot.

In conclusion, the exciton binding energies and the optical transition energies in $Ga_{0.9}In_{0.1}N/GaN$ and $Al_{0.395}In_{0.605}N$ /AlN quantum dots have been discussed with the inclusion of effects of geometrical confinement and the strain contributions. The same barrier height, for both the materials, has been taken in the problem. The largest intersubband optical transition energies of electron and heavy hole with the consideration of geometrical confinement have been dealt. The exciton oscillator strength as a function of dot radius in these quantum dots has been found. The interband optical absorption coefficients for a constant radius 20Å have been investigated. Also, the interband optical transition energies in the quantum dots have been obtained. We believe that the obtained results will pave the way to investigate further experimental research works on intersubband optical transitions in the mid infrared region towards the fabrication of light emitters, fiber optical telecommunication networks and the photo-detectors for spectroscopic applications based on the group-III nitride materials in near future.

References

Abbas, H. and Player, M. (2014), "Optical and electrical properties of undoped GaN films on sapphire substrate grown by metalorganic chemical vapor deposition", *Nat. Sci*., **12**(5), 80.

Ambacher, O., Majewski, J., Miskys, C., Link, A., Hermann, M., Eickhoff, M., Stutzmann, M., Bernardini, F., Fiorentini, V., Tilak, V., Schaff, W.J. and Eastman, L.F. (2002), "Optical detection of 2DEG in GaN/AlGaN structures - high magnetic field studies", *J. Phys. Cond. Matt*., **14**(13), 3399.

Ambacher, O., Majewski, J., Miskys, C., Link, A., Herman, M., Eickhoff, M., Stutzmann, M., Bernardini, F., Fiorentini, V., Tilak, V., Schaff, B. and Eastman, L.F. (2001), "Intersubband optical transitions in nitride based group-III semiconductor quantum dots", *J. Phys. Cond. Matt*., **14**, 3399.

Barve, A.V., Meesala, S., Sengupta, S., Kim, J.O., Chakrabarti, S. and Krishna, S. (2012), "Investigation of non-uniform electric field in intersubband quantum infrared photodetectors", *Appl. Phys. Lett*., **100**, 191107.

Bernardini, F., Fiorentini, V. and Vanderbilt, D. (1997), "Spontaneous polarization and piezoelectric constants of III-V nitrides", *Phys. Rev. B*, **56**(16), 10024.

Bhattacharya, P., Ghosh, S. and Stiff-Roberts, A.D. (2004), "Quantum dot optoelectronic devices", *Annu. Rev. Mater. Res*., **34**, 1.

Bigenwald, P., Lefebvre, P., Bretagnon, T. and Gil, B. (1999), "Confined excitons in GaN±AlGaN quantum wells", *Phys. Stat. Sol. B*, **216**, 371.

Bir, G.L. and Pikus, E. (1974), *Symmetry and Strain-Induced Effects in Semiconductors*, Wiley, New York.

Baer, N., Schulz, S., Schumacher, S., Gartner, P., Czycholl, G. and Jahnke, F. (2005), "Optical properties of self-organized wurtziteInN/GaN quantum dots: A combined atomistic tight-binding and full configuration interaction calculation", *Appl. Phys. Lett*, **87**, 231114.

Castrucc, P. (2014), "Nanotube-silicon heterojunction solar cells", *Adv. Nano Res*., **2**(1), 23.

Cao, J.C., Lei, X.L., Li, A.Z. and Liu, H.C. (2001), "Spectrum dynamics of negative-effective-mass

oscillators under a THz radiation", *Appl. Phys. Lett.*, **78**,2524.
de Sousa, J.S., Leburton, J.P., Freire, V.N. and da Silva, E.F. (2005), "Intraband absorption and stark effect in silicon nanocrystals", *Phys. Rev. B*, **72**, 155438.
Fonoberov, V.A. and Balandin, A.A. (2004), "Optical properties of wurtzite and zinc-blende GaN/AlN quantum dots", *J. Vac. Sci. Technol. B*, **22**, 2190.
Fonoberov, V.A. and Balandin, A.A. (2004), "Radiative lifetime of excitons in ZnO nanocrystals: the dead-layer effect", *Phys. Rev. B*, **70**, 195410.
Fonoberov, V.A. and Balandin, A.A. (2006), "ZnO quantum dots: properties andoptoelectronic applications", *J. Nanoelectro. Optoelectro*, **1**, 19.
Fonoberov, V.A., Alim, K.A., Balandin, A.A., Xiu, F. and Liu, J. (2006), "Photoluminescence investigation of the carrier recombination processes in ZnO quantum dots and nanocrystals", *Phys. Rev. B*, **73**,165317.
Haug, H. and Koch, S.W. (1994), *Quantum Theory of the Optical Properties of Semiconductors*, 3rd Edition, World Scientific, Singapore.
Köhler, R.R. *et al*. (2002), "Terahertz semiconductor-heterostructure laser", *Nature*, **417**, 156.
Koga, T., Nitta, J., Takayanagi, H. and Datta, S. (2002), "Spin-filter device based on the Rashba effect using a nonmagnetic resonant tunneling diode", *Phys. Rev. Lett*., **88**, 126601.
Kuhn, K.J., Lyengar, G.U. and Yee, S. (1991), "Nonlinear photonics: nonlinearities in optics, optoelectronics and fiber communication", *J. Appl. Phys*., **70**, 5010.
Liu, H.C. (1999), "Quantum well infrared photodetector physics and novel devices, Intersubband Transitions in Quantum Wells Physics and Device Applications", Eds. Weber, E.R. and Willardson, R.K., *Semiconductors and Semimetals*, **62**, Academic Press, San Diego.
Liu, H.C. *et al.* (2003), "Coupled electron-phonon modes in optically pumped resonant intersubband lasers", *Phys. Rev. Lett*., **90**, 077402.
Malis, O., Edmunds, C., Manfra, M.J. and Sivco, D.L. (2009), "Near-infrared intersubband absorption in molecular-beam epitaxy-grown lattice-matched InAlN/GaN superlattices", *Appl. Phys. Lett*., **94**, 16111.
Matthews, D.R., Summers, H.D., Smowton, P.M. and Hopkinson, M. (2002), "Ultrafast electron capture into p-modulation-doped quantum dots", *Appl. Phys. Lett*., **81**,4904.
Meighan, A., Rostami, A. and Abbasian, K. (2014), "Quantum computing using applied electric field to quantum dots", Adv. Nano Res., **2**(1), 15.
Nevou, L., Tchemycheva, M., Julien, F.H., Guillot, F. and Monroy, E. (2007), "Nano-semiconductors: devices and technology", *Appl. Phys. Lett*., **90**, 121106.
Nevou, L., Tchemycheva, M., Julien, F.H., Guillot, F., Monroy, E. and Sarigiannidou, E. (2008), "Intraband emission at lambda approximate to 1.48 μm from GaN/AlN quantum dots at room temperature", *Appl. Phys. Lett*., **92**, 161105.
Prete, P., Lovergine, N., Tapfer, L. and Mancini, A.M. (2001), "Structural properties of MOVPE-grown ZnMgSeepilayers and ZnSe/ZnMgSe MQWs on (100) GaAs", *Opt. Mater*., **17**, 207.
Qu, F. and Morais, P.C. (2003), "The optical stark effect in semiconductor quantum wires", *Phys. Lett. A*, **310**, 460.
Renard, J., Songmuang, R., Bougerol, C., Daudin, B. and Gayral, B. (2008), "Exciton and biexciton luminescence from single GaN/AlN quantum dots in nanowires", *Nanolett*, **8**(7), 2092.
Shi, J.J. and Gan, Z.Z. (2003), "Effects of piezoelectricity and spontaneous polarization on localized excitons in self-formed InGaN quantum dots", *J. Appl. Phys*., **94**, 407
Singh, J. (1996), *Optical properties of excitons in strained Gax In1-xAs/GaAs quantum dot: ef fect of geometrical conf inement on exciton g-factor, An Introduction to Materials and Devices, Optoelectronics*, Tata McGraw Hill, New Delhi.
Sun, K. *et al*. (2009), "Applications of colloidal quantum dots", *Microelectronics J*., **40**, 644.
Sun, H.H., Guo, F.Y., Li, D.Y., Wang, L., Wang, D.B. and Zhao, L.C. (2012), "Intersubband absorption properties of high Al content AlxGa1-xN/GaN multiple quantum wells grown with different interlayers by metal organic chemical vapor deposition", *Nanoscale Res. Lett*., **7**, 649.
Teleb, H., Abedi, K. and Golmohammadi, S. (2011), "Operation of quantum-dot semiconductor optical amplifiers under non-uniform current injection", *Appl. Opt*., **50**, 608.

Tchelidze, T. and Kereselidze, T. (2004), "Exciton energies and probability of their radiative decay in GaN/AlN quantum structures", *Opto-elect. Rev*., **12**(4), 441.
Voskoboynikov, O., Bauga, O., Lee, C.P. and Tretyak, O. (2003), "Magnetic properties of parabolic quantum dots in the presence of the spin–orbit Interaction", *J. Appl. Phys.*, **94**, 5891.
Vurgaftman, I., Meyer, J.R. and Ram-ohan, L.R. (2001), "Band parameters for III-V compound semiconductors and their alloys", *J. Appl. Phys.*, 89, 5815.
Wang, G., Duan, X. and Chen, W. (2013), "Application and performance of 3d printing in nanobiomaterials", *Nanomat*., Article ID 240563.

CC